Swelling of high acyl gellan gum hydrogel

Kanyuck, K. M.; Mills, T. B.; Norton, I. T.; Norton-Welch, A. B.

DOI:
10.1016/j.carbpol.2021.117758

Document Version
Peer reviewed version

Citation for published version (Harvard):
Kanyuck, KM, Mills, TB, Norton, IT & Norton-Welch, AB 2021, 'Swelling of high acyl gellan gum hydrogel: characterization of network strengthening and slower release', *Carbohydrate Polymers*, vol. 259, 117758. https://doi.org/10.1016/j.carbpol.2021.117758

Swelling of High Acyl Gellan Gum Hydrogel: Characterization of Network Strengthening and Slower Release

K. M. Kanyuck*, T. B. Mills, I. T. Norton, A. B. Norton-Welch

School of Chemical Engineering, University of Birmingham, Edgbaston, Birmingham, B15 2TT, UK

*Contact information for the corresponding author: Kelsey Kanyuck. Tel: +44 121 414 5364 Email: KXK720@student.bham.ac.uk

Abstract

This study examined the mechanism of swelling for high acyl (HA) gellan gum and the impacts on the hydrogel mechanical properties and the release of a model drug (glucose). Controlling the material properties and the release of entrapped drugs during use in aqueous environments, such as the stomach or bodily fluids, are crucial in designing functional applications. Swelling of HA gellan gum was controlled by varying the osmotic environment with salts and solvents, and effects on the gel network were characterized by uniaxial compression tests, DSC, and rheology. Low ionic strength solutions caused the greatest degree of swelling (up to 400%) and corresponded to a more brittle gel with a greater modulus and greater network enthalpy. Swelling slowed the release of glucose by decreasing the diffusion flux. The osmotic environment was found to produce different functional properties, and it is crucial to consider these changes in the design of formulations.

Keywords: gellan gum; swelling; drug release; gellan hydrogel**;** tissue scaffold; superabsorbent hydrogel

1. Introduction

Hydrocolloid gels are frequently used to create soft-solid structures composed predominately of water in the food, pharmaceutical, and tissue engineering industries. Gellan gum is a carbohydrate hydrocolloid that forms physical gels and is commonly used in each of these industries (Coutinho et al., 2010; Morris, Nishinari, & Rinaudo, 2012; Osmałek, Froelich, Jadach, & Krakowski, 2018; Palumbo, Federico, Pitarresi, Fiorica, & Giammona, 2020; Stevens, Gilmore, & Wallace, 2016). Cytocompatibility, easy processability, mucoadhesion, tuneable mechanical properties, and food-grade status offer many attractive benefits for using gellan gum (Morris, Nishinari, & Rinaudo, 2012; Palumbo, Federico, Pitarresi, Fiorica, & Giammona, 2020; Stevens, Gilmore, & Wallace, 2016). There are two types of gellan gum available: the native or high acyl (HA) and a modified version termed low acyl (LA). The repeating unit of LA gellan gum is →3)-β-D-glucose-(1 → 4)-β-D-glucoronic acid-(1 → 4)-β-D-glucose-(1 → 4)-α-L-rhamnose-(1→ and HA gellan gum has additional substitutions of glyceryl and acetyl units on the 3-linked glucose (Supplementary Figure 1) (Morris, Nishinari, & Rinaudo, 2012; Sworn, 2009).

Both gellan variants form gels by a helix-coil transition occurring upon cooling (after dispersing in hot water 80-90 °C) (Morris, Nishinari, & Rinaudo, 2012). The acetate group on the HA gellan polymer prevents aggregation of double helix chains and follows a fibrous gelation model through end to end associations (Morris, Gothard, Hember, Manning, & Robinson, 1996; Morris, Nishinari, & Rinaudo, 2012). The removal of acyl groups from HA gellan yields a completely different gel texture in LA from modification to the helix structure and aggregation mechanism. HA gellan forms a soft and easily deformable gel, while the gel of LA gellan is firm and brittle (Morris, Nishinari, & Rinaudo, 2012). LA gellan requires monovalent cations to promote double helix formation and divalent cations to allow aggregation of helices, while the HA gellan gelation does not require salt (but it does promote gelation) (Mazen, Milas, & Rinaudo, 1999; Miyoshi & Nishinari, 1999). Recent studies have demonstrated that aggregates of HA gellan, created during the drying process, contribute to the

shear storage modulus (Shinsho et al., 2020). Additional reports suggested a heterogeneous gel structure with crystalline regions and amorphous regions (Yang et al., 2019) presumed to be the helices and aggregates respectively.

The response of gellan gum gels to submersion into aqueous solutions is of interest in both the pharmaceutical and food industries for examining digestion (Lin & Metters, 2006; Norton, Hancocks, & Grover, 2014) and tissue engineering for response to body conditions (De Silva, Poole-Warren, Martens, & in het Panhuis, 2013; Pereira et al., 2011). A common property of charged gel networks, including gellan, is the uptake of water to increase the volume and mass of the gel (defined as swelling). Theory of polymer swelling postulates three driving causes of swelling: polymer-solvent interactions, elasticity, and Donnan potential (Annaka, Ogata, & Nakahira, 2000; Sakai, 2020). Elastic pressure holds the gel network together while the Donnan potential and polymer-solvent interactions drive dissolution. The equation proposes the total osmotic pressure (Π) causing swelling for a charged gel is driven by the summation of polymer-solvent mixing (Π_{mix}), chain elasticity ($\Pi_{elastic}$), and Donnan potential ions (Π_{ion}) (Annaka, Ogata, & Nakahira, 2000; Sakai, 2020):

$$\Pi = \Pi_{mix} + \Pi_{elastic} + \Pi_{ion} \quad \text{(Eq. 1)}$$

For charged gels with complexed counter ions, the Donnan potential is the greatest influence. Higher concentrations of counter ions inside the gel and low concentration of ions in solutions (in the case of DI water) drives water into the gel (Annaka, Ogata, & Nakahira, 2000; Coutinho et al., 2010). The maximum swelling is limited by the crosslink density (Moe, Elgsaeter, Skjåk-Bræk, & Smidsrød, 1993) and the extent depended on the osmotic gradient (Annaka, Ogata, & Nakahira, 2000; Coutinho et al., 2010).

Large increases in the mass of HA gellan gels have been reported upon submersion in aqueous environments (Cassanelli, Norton, & Mills, 2018b; Chen et al., 2020; de Souza, de Mello Ferreira, I. L., da Silva Costa, M. A., da Costa, M. P. M., & da Silva, 2021; Liu, Wang, Gao, & Bai, 2013). In water, a 2% HA gellan gel increased in mass by 192% (Cassanelli, Norton, & Mills, 2018b). Swelling of freeze

dried HA gellan gum gels have been measured, but it is known the freeze drying process partially destroys the gel structure (Cassanelli, Norton, & Mills, 2018a) so a true comparison cannot be made. Increases in mass ranged from 1,150% to 32,000% for the freeze dried gel (Chen et al., 2020; de Souza, de Mello Ferreira, I. L., da Silva Costa, M. A., da Costa, M. P. M., & da Silva, 2021; Liu, Wang, Gao, & Bai, 2013). In simulated body conditions (typically high salt), both increased (De Silva, Poole-Warren, Martens, & in het Panhuis, 2013; Osmałek, Froelich, Jadach, & Krakowski, 2018) and decreased (Osmałek, Froelich, Jadach, & Krakowski, 2018; Pereira et al., 2011) modulus have been observed but none of these looked at the effect of ion concentration on the swelling.

Swelling of modified LA gellan gum gels was driven by salt concentration (Annaka, Ogata, & Nakahira, 2000; Coutinho et al., 2010). An increased modulus was observed from submersion of LA gellan in salt solutions (De Silva, Poole-Warren, Martens, & in het Panhuis, 2013; Hossain & Nishinari, 2009; Nitta, Ikeda, & Nishinari, 2006; Tanaka & Nishinari, 2007; Yu, Kaonis, & Chen, 2017), acidic solutions (Norton, Hancocks, & Grover, 2014), and even DI water (Hossain & Nishinari, 2009; Nitta, Ikeda, & Nishinari, 2006). It was thought to arise from aggregation of unaggregated helices by the additional counter ions (De Silva, Poole-Warren, Martens, & in het Panhuis, 2013; Hossain & Nishinari, 2009; Nitta, Ikeda, & Nishinari, 2006; Tanaka & Nishinari, 2007; Yu, Kaonis, & Chen, 2017). The hypothesis of ions migrating from an external solution during soaking and causing this further aggregation has been generally accepted (Morris, Nishinari, & Rinaudo, 2012). The behaviour of hardening in DI water has also been observed but cannot be explained by the cation theory (Hossain & Nishinari, 2009; Nitta, Ikeda, & Nishinari, 2006). Hossain and Nishinari (Hossain & Nishinari, 2009) proposed that the swelling caused “stiffening of network chains” which led to the increased modulus but no further analysis or mechanism was given. The behaviour of HA gellan may provide additional understanding because it does not aggregate through counterions, but no comparison has yet been made.

Lack of a fundamental understanding of HA gellan swelling and the interesting swelling-hardening of LA gellan necessitate further examination to understand gellan gum behaviour. No studies have comprehensively examined the origin of HA gellan swelling or the structural changes taking place during swelling. Several researches have highlighted the need to examine changes in material properties during usage in aqueous solutions (Stevens, Gilmore, & Wallace, 2016; Yu, Kaonis, & Chen, 2017). This work will investigate the mechanism of swelling of HA gellan gum, the effects of swelling on the network structure, and the impact on release of a small molecule. This work hypothesized that HA gellan swelling is driven by an osmotic imbalance which causes a rearrangement of chains to an extended structure and is accompanied by a physical strengthening to the network. Swelling of HA gellan gum gels was controlled by altering salt concentration gradients and the resulting physical properties and network structure were examined. Additionally, the effects of solvent properties were compared to elucidate mechanisms for the physical change. Lastly, release of glucose from gellan gels under high-swelling and low-swelling environments were compared to determine the impact of swelling.

2. Materials and Methods

2.1. Materials

HA (LT100) and LA (F) gellan gum were acquired from CP Kelco (Atlanta, USA). The linear polymer is comprised of a repeating sequence of a β-D-glucose, one β -D glucoronate, one β -D-glucose, and one α-L-rhamnose and the chemical structure shown in Supplementary Figure 1 (Morris, Nishinari, & Rinaudo, 2012; Sworn, 2009). HA gellan has acetyl and glyceryl substitutions on the first glucose of the repeating unit at O(2) and O(6) respectively while the acyl groups are removed for LA gellan gum (Morris, Nishinari, & Rinaudo, 2012). The total degree of acylation for LT100 indicated a glycerate group on 90% of those units and an acetyl group on 40% of the units (Kasapis et al., 1999). The molecular weight of HA gellan gum is 1-2 x 10^6 Da and LA gellan gum is 2-3 x 10^5 Da (CP Kelco specifications; Shinsho et al., 2020). Further characterization of this polymer by FTIR and NMR has

been published by de Souza et al. (2021). Cations present within the commercial gellan gums were analysed by ICP-OES (Optima 8000 by PerkinElmer, Waltham, USA). Counterions of the HA gellan powder were predominately potassium and contained 19,000 ppm K+, 3,600 ppm Na+, 2,200 ppm Ca^2+ and below LoQ of Mg^2+. Similarly, the LA gellan was also +potassium-type and contained 46,000 ppm K+, 6,300 ppm Na+, 1,400 ppm Ca^2+ and 580 ppm Mg^2+. Materials were used as described without any further purification. The DI water was prepared with a reverse osmosis milli-Q water system (Merck, Kenilworth, USA). On the logarithmic plots, DI water is considered as 0.0001 mM salt to allow it to be within the bounds of the x-axis. Solutions were prepared from salts (KCl and NaCl, $CaCl_2$) and glucose and purchased from Sigma Aldrich (St. Louis, USA).

2.2. Sample preparation

All gels were prepared by dispersing the hydrocolloid powder at 2% w/w in 90 °C DI water with stirring for two hours to hydrate the polymers. Samples used for glucose released were prepared at 4% and mixed with an 80° C glucose solution (at 60%) prior to the cooling and setting of the gel (they were mixed as two solutions). A final concentration of 30% glucose and 2% gellan gum was achieved. Hot solutions were poured into 20mm diameter cylindrical plastic moulds and set at room temperature (20°C ± 1°C) for at least 24 hours before analysis. All samples were prepared in at least triplicate and error bars represent standard deviation.

Solvent properties were examined by submerging gels in solutions of DI water with added ethanol, glucose, or glucose with KCl. The 'solvent %' refers to the amount of ethanol or glucose added to the mixture on a total weight ratio. The samples with glucose and KCl were each formulated at a final concentration of 100 mM. All solutions were prepared 24 hours before usage.

2.3. Swelling measurement

Swelling of gellan gum gels was measured by increases in mass after soaking in aqueous solutions. Gels were cut into ~20 mm height pieces from the cylindrical moulds (20 mm diameter) and the

mass of 7.5 g ± 1 g weighed. The gel was then placed into 150 mL of solution at room temperature. Salt concentrations of the solutions ranged from 0.0001 mM to 1000 mM as indicated in each figure. After 48 hours the gel was removed using a strainer, pat dry to remove surface water, and weighed. Swelling was quantified using the ratio of initial mass to final mass by the equation where M is the measured sample mass after swelling and M_0 is the initial mass:

$$\text{Swelling Ratio } (q) = M/M_0 \qquad \text{(Eq. 2)}$$

This parameter was proposed by Djabourov (Djabourov, Nishinari, & Ross-Murphy, 2013) and chosen to mimic the values used during release studies. Distinction should be made from another common swelling ratio 'Q' which measures the swelling of a freeze dried gel. As it is known the process of freeze drier partially destroys the gellan network (Cassanelli, Norton, & Mills, 2018a), these gels were not freeze dried prior to measurement. Comparison to values obtained from freeze-dried samples are not equivalent.

2.4. Gel compression and fracture

A compression test was used to measure the physical properties of fresh and swollen gels with a TA.XT.plus Texture Analyser (Stable Micro Systems, Godalming, UK). Analysis was completed immediately after the 48 hour period of submersion. Prior to submersion in the water, all samples had dimensions of 20 mm diameter and 20 mm height. Upon swelling, these dimensions changed. For gels that had swelled, the new radius was measured and accounted for in the calculations and the height was cut to maintain a constant 20 mm. The compression used two parallel plates which were both larger than the dimensions of the sample. Gels were placed on the bottom plate and the upper plate was moved downward at 2 mm/s until fracture occurred. Sample height was recorded during the experiment, and the surface area was calculated by measuring diameter of each individual sample. The Young's modulus was determined by the slope of the initial linear relationship between stress and strain. True stress and true strain were calculated to account for the changing dimensions of the gel during compression.

2.5. Differential Scanning Calorimetry (DSC)

Changes in enthalpy and entropy of the gel from submersion in water were analysed with DSC. The instrument was a μDSC3evo by Setaram Instrumentation (Caluire, France) which feature sample cell tubes with ~0.9 mL volume made of Hastelloy and able to be tightly sealed (up to 20 bar). Samples were prepared by cutting cylindrical pieces from the gels to fill the samples cells with 750 mg ± 50 mg. Identical mass of DI water was added to the reference cell within ± 10 mg. Thermograph cycles began with a hold at 5 °C for 10 minutes and then increased at 1 °C/min up to 95 °C. After a 10 minute hold at 95 °C, the temperature was cooled at 1 °C/min down to 5 °C (to be referred to as the first run). This cycle was repeated again immediately after and termed the second run. Gels were prepared and analysed at least 4 separate times for each sample.

2.6. Rheology

Oscillatory rheology was performed with a Kinexus Rheometer (Malven Panalytical Ltd, Malvern, UK) using a 20 mm parallel plate geometry. Circular slices of a 20 mm diameter were carefully cut to a height of 1.5-2.5 mm and placed directly on the geometry. Differing height between samples was accounted for by loading to a normal force between 0.2 and 0.3 N so the gap ranged from 1.5 mm to 2.5 mm. A strain sweep was conducted from 0.01% to 100% at a frequency of 1 Hz and a temperature of 20 °C and all samples had a linear viscoelastic region (LVER) greater than 1%. Prior to conducting the temperatures sweeps the temperature was held constant for 5 minutes at 5° C to allow equilibration and following was raised at 1 °C/min from 5 °C to 90 °C. A frequency of 1 Hz and a strain of 0.1% was used. Three replicates were analysed for each sample and error bars show the standard deviation.

2.7. Release

To compare release of a small molecule (glucose) from gels, a model system was used. Gels were placed into 150 mL of aqueous solution (DI water or 50 mM KCl) at 37 °C to mimic body temperature. A shaker with 200 RPM was used for mixing the bulk solution and the gels were held in place with dialysis tubing. Gels were prepared with 30% glucose and set for 24 hours prior to measurement (section 2.2). Before analysis, gels were cut into 1 mL pieces (1 cm height) and four were utilized in each release experiment (5 g total). The concentration of glucose in the aqueous solution was measured at each time point with a refractometer (Rudolph Research J357 automatic refractometer from Hackettstown, USA). For every sample, the release after 24 hours was 100 ± 5% of the expected glucose concentration and thus values were normalized to the maximum release to minimize the effect of sample variability.

3. Results and Discussion

3.1. Swelling of gellan gum

Submersion of gellan gels into water caused enlargement of the network and an absorption of water resulting in a higher mass. Swelling of HA gellan and LA gellan are shown over the course of 7 days in Figure 1 and additional data is shown in Table 1. HA gellan had a much greater swelling ratio than for LA gellan and both had greater swelling in DI water than in 50mM KCl. Neither gellan appeared to reach a single equilibrium swelling value, with HA gellan continuing to increase while LA gellan began to decrease after 180 minutes (Table 1). For LA gellan gum, the maximum swelling ratio was reached at 180 minutes while HA gellan continued to increase logarithmically up to 14 days. In agreement with previous work, the maximum swelling of LA gellan occurred between 120 and 180 minutes (Nitta, Ikeda, & Nishinari, 2006). An initial structural rearrangement was followed by a low degree of dissolution of polymer chains for LA gellan in DI water. The absence of HA gellan gum dissolution in DI water was interesting. These differences in apparent equilibrium likely reflect the essential participation of cations in the gelation of LA gellan but not HA gellan.

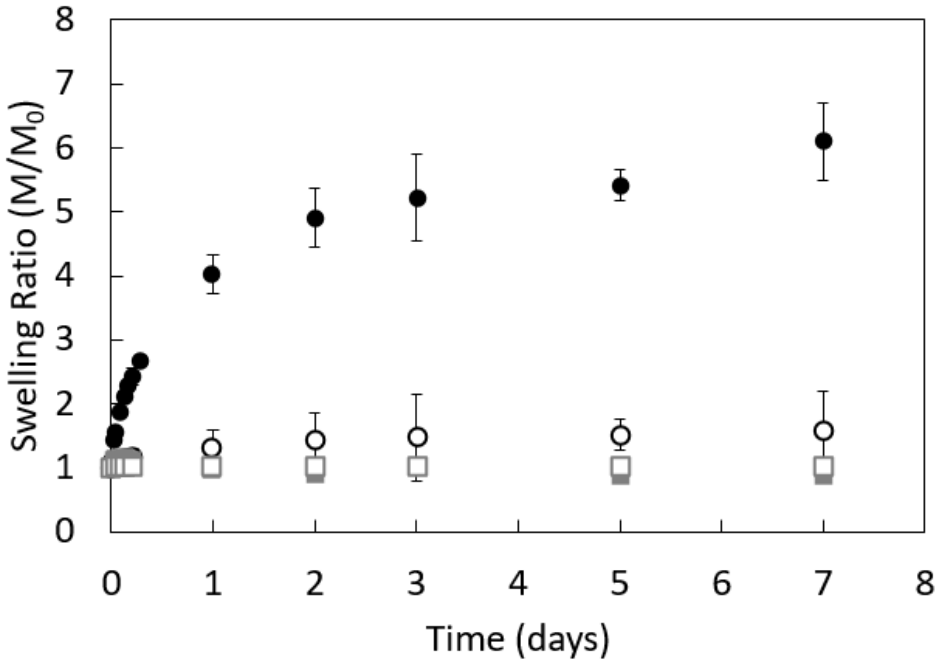

Figure 1. Changes in swelling ratio of 2% high acyl (HA) gellan (●) and low acyl (LA) gellan (■) during submersion in DI water (filled symbol) and in 50 mM KCl (unfilled symbol ○ and □) for up to 7 days at room temperature.

Table 1. Swelling ratio of high acyl (HA) gellan and low acyl (LA) gellan gum gels after submersion in 150mL of solution the indicated solution. Averages are reported with ± the standard deviation.

	60 mins	**120 mins**	**180 mins**	**24 hours**	**2 days**	**7 days**	**14 days**
2% HA gellan gum in DI water	1.57 ± 0.06	1.87 ± 0.06	2.11 ± 0.09	4.03 ± 0.3	5.03 ± 0.4	6.10 ± 0.6	7.10 ± 0.6
2% HA gellan gum in 50mM KCl	1.09 ± 0.01	1.12 ± 0.02	1.14 ± 0.01	1.31 ± 0.02	1.42 ± 0.01	1.59 ± 0.03	1.66 ± 0.03
2% LA gellan gum in DI water	1.15 ± 0.02	1.15 ± 0.06	1.19 ± 0.02	0.99 ± 0.02	0.91 ± 0.05	0.86 ± 0.04	0.82 ± 0.03
2% LA gellan gum in 50mM KCl	1.03 ± 0.01	1.04 ± 0.004	1.05 ± 0.003	1.04 ± 0.004	1.03 ± 0.003	1.04 ± 0.01	1.04 ± 0.01

The unique ability for HA gellan to increase in size by 400%, without indication of chain dissolution, was of particular interest. A practical time point of 2 days after submersion in water was chosen for future measurements, when the change appeared to slow for HA gellan, although this does not represent a true equilibrium value. Characterization of this swelling by controlling solution properties and measuring the resulting structural and mechanical properties were the subject of this research.

3.2. Ionic influence on HA gellan gum swelling

Swelling is driven by the total osmotic contribution (Π) and is a combination of polymer-solvent mixing (Π_{mix}), chain elasticity ($\Pi_{elastic}$), and the Donnan potential (Π_{ion}) for charged polymers (Eq. 1). Helix formation is assumed to be unchanged by the swelling and instead causes a tertiary rearrangement of the polymer. A change in the hydrodynamic volume would be reflected in Π_{mix}. The existing gel network resists swelling by $\Pi_{elastic}$ and acts to hold the gel together. Cationic polymers are well known to swell from a high Π_{ion} if the salt concentration outside the gel is lower than inside the gel (Annaka, Ogata, & Nakahira, 2000). The term swelling has sometimes been be used to describe the change from a compact rigid polymer in a glassy state to an extended large pored rubbery network (Lin & Metters, 2006), however in this work the transition is from a soft loose network to a more rigid and extended network. Both cases involve an increased proportion of water per unit of polymer, but with differing effects on the material properties.

The following experiments will control for the Donnan contribution (Π_{ion}) to examine the effect of swelling on the HA gellan gum gel network. Effects of external ionic concentration on the swelling of a 2% HA gellan gel are shown in Figure 2. In DI water and low concentrations of chloride ions (0.01 mM and below), the swelling ratio of 2% HA gellan was at a maximum of 5.0 (Figure 2 zone 1). Sigmoidal shape of the curve was consistent with Donnan equilibrium (whereby swelling is caused from an imbalance of ions inside and outside the gel) and also supported by the similarity of the ions (Annaka, Ogata, & Nakahira, 2000). The end of the linear portion of the sigmoid and beginning to

248 approach an asymptote (between 10 and 50 mM) is thought to be the equivalence point. Here the
249 internal ionic concentration is likely equal to the outside concentration and would correspond to a
250 Donnan effect of near zero (Figure 2 zone 2). Calculating the internal gel ionic concentration from
251 the ICP data (section 2.1) estimates a 15 mM cationic concentration (10 mM for K+ alone) in a 2%
252 gel. Falling between these two concentrations (of 10 and 50mM), the measured values are
253 consistent with an expected equivalence point (15 mM). High ionic concentrations in the external
254 solution (above 50 mM) and the Donnan effect alone should actually promote deswelling (swelling
255 ratio lower than 1 and a loss of water from the gel). In this region, contributions from Π_{mix} must
256 cause a net positive swelling force. Not until 1,000 mM KCl does the swelling ratio drop below one
257 (Figure 2).

258 Contribution of the Donnan effect to the total swelling was estimated by comparing the maximum
259 swelling ratio (5.0) to the ionic balanced swelling (1.4). A large proportion (90%) of the swelling in DI
260 water was consistent with osmosis-driven salt imbalance. The other 10% of swelling is likely a
261 contribution from Π_{mix} (Eq. 1). For LA gellan, a comparable salt dependant swelling has been
262 previously established (Annaka, Ogata, & Nakahira, 2000; Coutinho et al., 2010; Nitta, Ikeda, &
263 Nishinari, 2006). In addition to the increase in mass of 400% from the Donnan effect, soaking gellan
264 in water also led to a network strengthening that could not be explained by the change in
265 concentration.

266 **3.2.1. Mechanical properties**

267 Mechanical properties of these swollen gels were compared using uniaxial compression testing to
268 measure the Young's Modulus (Figure 3) and the strain to fracture (Figure 4). Submerging HA gellan
269 gels in aqueous solution caused an increase in modulus (Figure 3) but interestingly was not directly
270 related to the swelling (R^2 = 0.11). Whether in DI water or up to 10 mM KCl, the higher modulus was
271 consistent (13 kPa ± 0.8 kPa) while the swelling ratio ranged from 5.0 to 1.9 (Figure 2). At
272 concentrations of salt greater than 50 mM, there was an increasing modulus predicted to be caused

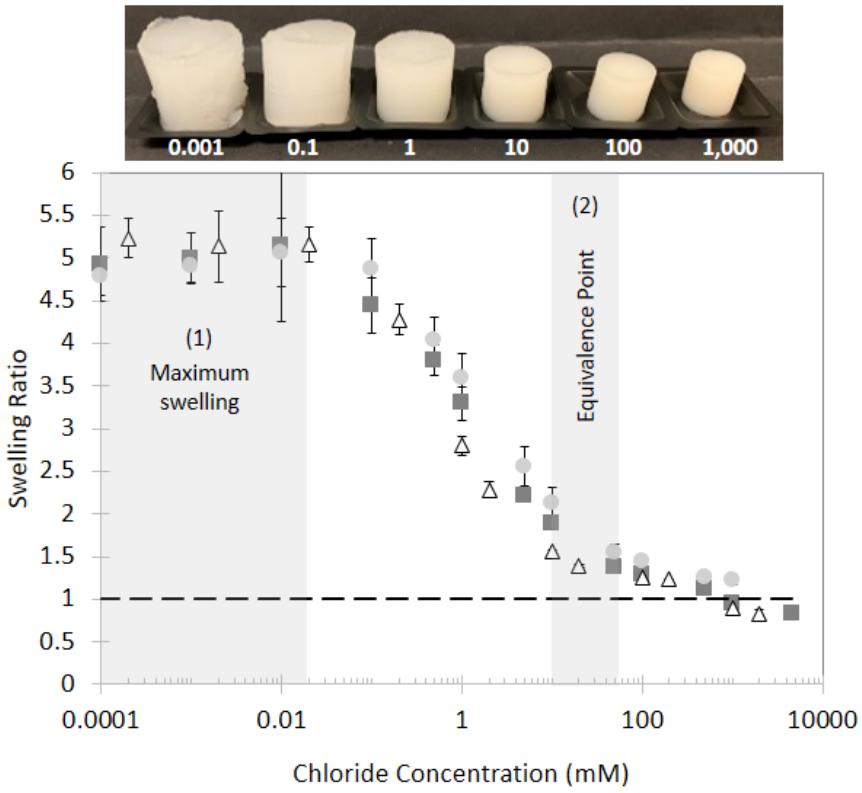

Figure 2. Influence of salt concentrations on swelling of 2% high acyl gellan gels after soaking in 150mL of the indicated solution of KCl (■), NaCl (●), and $CaCl_2$ (Δ) for 48 hours and images show the change in appearance for gellan soaked in KCl solutions. Maximum swelling occurred in zone 1 and the equivalence salt concentration was estimated between 10 and 50 mM salt in zone 2.

from 'salting-out' which is common for hydrocolloids at high ionic strengths. The lowest modulus of the soaked samples occurred in the equivalence salt (zone 2) where the modulus was similar to the fresh (not soaked) gellan gel. The increase in modulus at low ionic concentrations cannot be attributed to an increase in polymer or counter ion concentration as both parameters actually decreased during the swelling. Modulus increases at high degrees of swelling has been explained by a deviation from Gaussian behaviour caused from extensive stretching of the polymer chains (Djabourov, Nishinari, & Ross-Murphy, 2013; Skouri, Schosseler, Munch, & Candau, 1995). Additionally, it is possible new bonds were formed during swelling which will be examined by DSC in a following section.

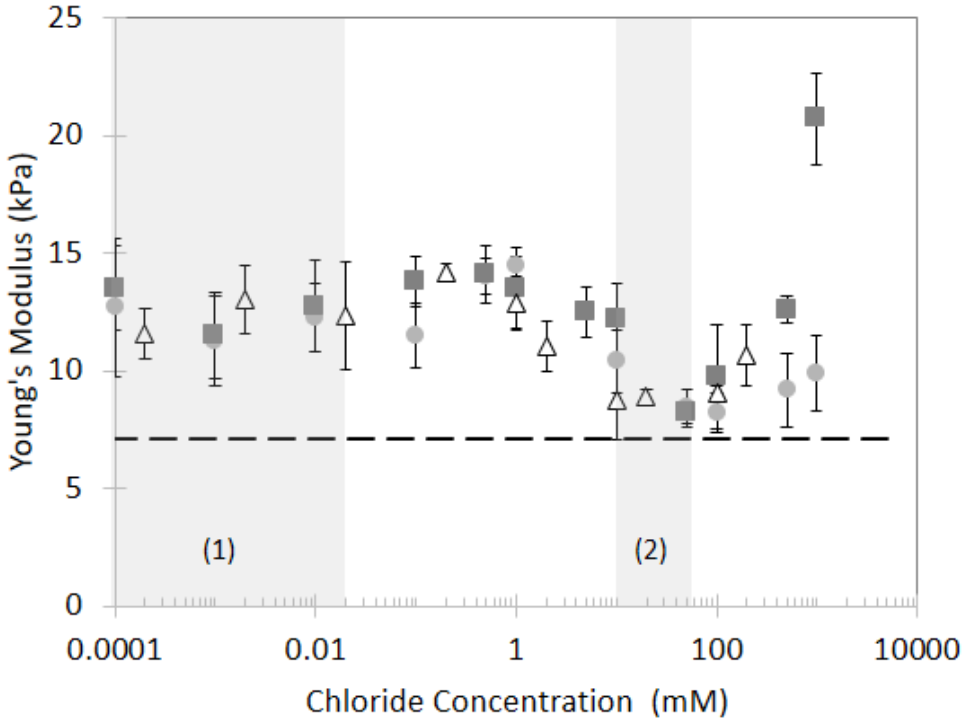

288

289 **Figure 3**. Influence of ionic effect on the Young's Modulus of 2% high acyl gellan gels after soaking in
290 150mL solutions of KCl (■), NaCl (●), and $CaCl_2$ (▲) compared to a fresh sample (dotted line) for 48
291 hours. Maximum swelling occurred in zone 1 and the equivalence salt concentration was estimated
292 between 10 and 50 mM salt in zone 2.

293

294 Strain to fracture of swollen gels was well correlated (R^2 = 0.96) to the ratio of swelling (Figure 4).
295 Images of the compressed and fractured gels are shown in (Figure 4). Water removal from gels
296 during compression (like a sponge) was not observed from the HA gellan gels as previously reported
297 for the LA gellan variant (Nakamura, Shinoda, & Tokita, 2001). The increased brittleness of gels (with
298 a lower strain to fracture) appears to be caused by the extension of polymer chains during swelling.
299 As swelling causes the network to expand, space between junction zones must get larger and the gel
300 more rigid, thus forming a network less able to deform without fracture.

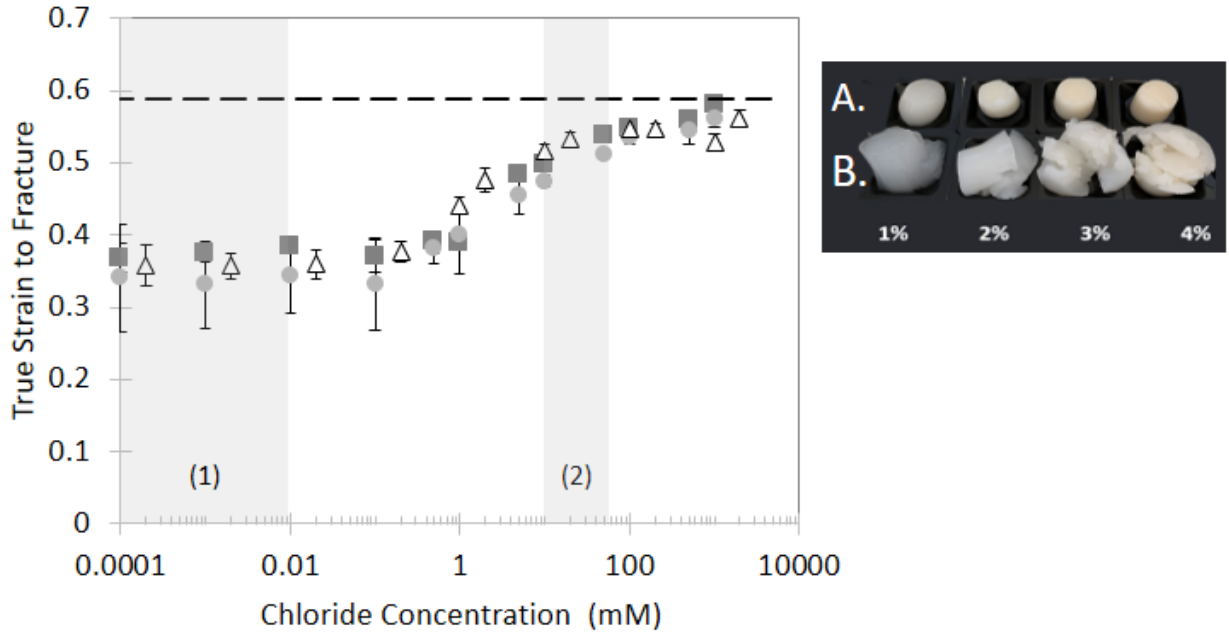

Figure 4. Changes in gel fracture of 2% high acyl gellan after soaking in 150mL of of KCl (■), NaCl (●), and $CaCl_2$ (Δ) compared to a fresh sample (dotted line). Maximum swelling occurred in zone 1 and the equivalence salt concentration was estimated between 10 and 50 mM salt in zone 2. Image shows the appearance of HA gellan gum gels at the indicated concentration (A) before treatment and (B) fractured gels after soaking in DI water.

Previous measurement of the change in modulus of soaked HA gellan gels did not account for the salt concentration. For a 2% HA gellan gel, De Silva et al. (De Silva, Poole-Warren, Martens, & in het Panhuis, 2013) found no change in the Young's Modulus or strain to fracture for a gel submerged in PBS for up to 14 days. Both an increase and a decrease in modulus were observed for a 0.4% HA gellan in a comparison of different bodily fluids (Osmałek, Froelich, Jadach, & Krakowski, 2018). Applying the effect of ionic concentration from the current work, the discrepancy between these authors work likely originates from differing ionic strengths.

Here there are likely two factors at play in changes to the modulus with the varying ionic strengths: Donnan effect swelling and salting out of the polymer. Between 0 and 10mM the changes are driven

by an ionic-imbalance salt swelling (the Donnan effect). This range is characterized by high swelling, increased modulus, and the most brittle gels. The range from 0.1 to 10mM is roughly the linear region of the sigmoidal curve where the greatest change in swelling ratio with salt was observed (largest slope). The modulus did not vary with swelling ratio. Between 10 and 50mM was the equivalence point of ionic concentration inside and outside the gel. Swelling ratio at this point is not zero though, as swelling was still driven by the other contributions (Equation 1). At the ionic equivalence point, the Young's Modulus is at a minimum. Matching the internal and external solution properties resulted in the smallest changes from the original gel. At even higher ionic concentrations (greater than 100 mM), salting-out of the polymer likely had caused the increased modulus. Molecular origins of this higher modulus at low ionic strength (<10 mM) were examined next.

3.3. Characterization of gel network changes

The increased gel strength observed upon submersion in low ionic strength solutions was hypothesized to be caused by hydrophobic-driven helix formation. A low correlation to the swelling itself (R^2 = 0.11) suggested an alternative mechanism to just "stiffening of chains" as proposed for the LA gellan (Hossain & Nishinari, 2009). The effective concentration was lower and the salt concentration was lower; both of these are typically thought to drive gelation. Therefore a different mechanism must have caused the increased modulus. First, the networks of swollen and standard gels were compared with DSC and then mixed solvents were compared to understand solubility characteristics of the gels.

3.3.1. DSC

To examine changes in the network during swelling of gels, fresh (no soaking in water) and swollen gels were examined by DSC. Thermographs of the heating curves are shown in Figure 5 and the enthalpy and transition temperatures are shown in Table 2. Enthalpies were normalized to the weight of the polymer to account for the differences in concentration between the swollen samples

342 and fresh gel. An endothermic peak between 65 and 76 °C is known to be the helix coil transition of
343 HA gellan gum (Huang, Singh, Tang, & Swanson, 2004; Mazen, Milas, & Rinaudo, 1999; Murillo-
344 Martínez & Tecante, 2014). A peak representing this helix to coil transition was observed for each of
345 the samples with some variation in melting temperature due to the differences in salt. Ionic
346 concentration is well known to effect the gelation temperature of HA gellan gum (Flores-Huicochea,
347 Rodríguez-Hernández, Espinosa-Solares, & Tecante, 2013; Huang, Singh, Tang, & Swanson, 2004;
348 Mazen, Milas, & Rinaudo, 1999). The decreased melting temperature of the sample soaked in DI
349 water was indicative of the lower salt environment. Alternatively, soaking in 50 mM KCl resulted in a
350 higher melting temperature (4 °C). This concentration was an estimation of the equivalent
351 concentration (between 10 and 50mM KCl) and in practice the selected 50mM KCl was marginally
352 higher than the gel itself. The higher melting temperature was a reflection of this greater salt.

353 Comparing enthalpies of melting for gel networks gives an indication of internal energy associated
354 with the helix coil transition. Differences in melting temperature were taken into consideration by
355 calculating the entropy and Gibbs free energy (ΔG) associated with each melting event. In the
356 soaked samples there was considerable sample to sample variability in temperature (suggested by
357 the large error bars). The μDSC technique utilizes only a small (~750 mg) portion of sample and this
358 high variability would be consistent with heterogeneity within the gel. Due to the lack of helix
359 aggregation, there is little cooperation between helicies and DSC peaks are normally wide (Morris,
360 Nishinari, & Rinaudo, 2012). Gels soaked in DI water resulted in greater enthalpy and ΔG compared
361 to a fresh gel (enthalpy of 45 J/g compared to 27 J/g from Table 2 $p < 0.05$). Soaking in 50 mM KCl
362 did not result in a significant change in the enthalpy ($p > 0.05$) but did cause an increase in ΔG
363 compared to the fresh gel. The greater ΔG could be explained by the greater salt content (Mazen,
364 Milas, & Rinaudo, 1999). Generally, salt environments can be expected to drive further helix
365 crosslink formation (Mazen, Milas, & Rinaudo, 1999). The same is not expected of submersion in DI

366

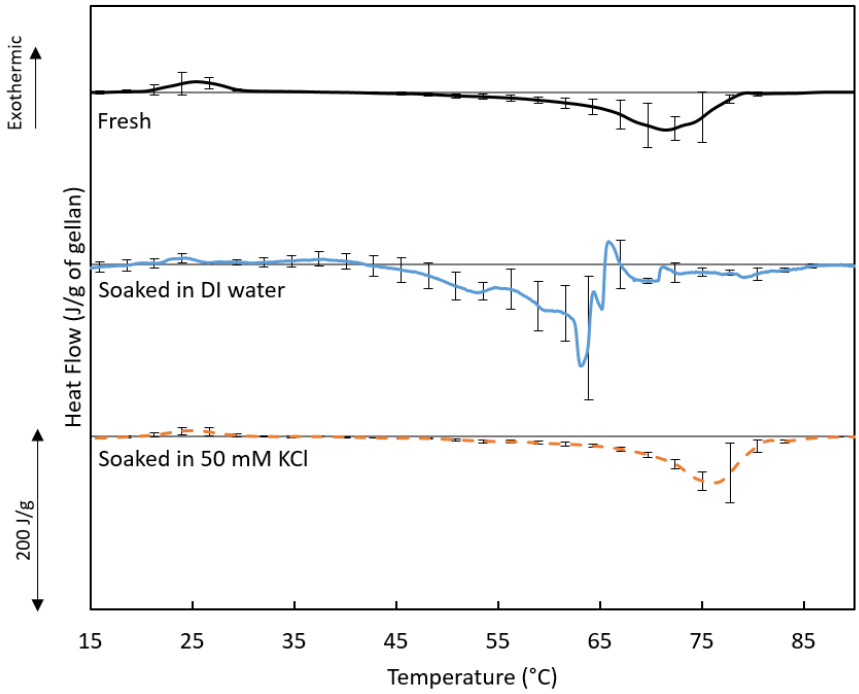

Figure 5. DSC heating thermographs for 2% high acyl (HA) gellan gum fresh (without any treatment) and after soaking in deionized (DI) water or 50 mM KCl for 48 hours. Swelling took place outside of the DSC cells and changes in HA gellan concentration were accounted by normalizing to total the polymer weight in each sample. Error bars represent the standard deviation of five replicates where the deviation was mainly from differences in temperatuare ranges for 'soaked in DI water' and differences in area between 'fresh' and 'soaked in 50mM KCl' samples.

water. The process of swelling and the lower salt environment appeared to decrease the solubility of HA gellan and drive helix formation. These new bonds may have been the cause of the network strengthening (increased modulus) observed during swelling. Alternatively, extensive stretching of chains, past the point of a Gaussian assumption, has also led to a higher modulus (Skouri, Schosseler, Munch, & Candau, 1995). Although the enthalpy of HA gellan (per gram) increased during swelling, the effective concentration decreased by 4-5x causing much complexity for assigning an origin of behaviour. It is likely that both factors were influential in the change of modulus.

Table 2. Enthalpy of melting (J/g of polymer) and peak melting temperatre (°C) for 2% high acyl gellan gum from Figure 5 and calculated entropy and Gibbs free energy (ΔG). Values were normalized to the grams of gellan in each sample and are reported as the average with one standard deviation. Means were compared for each column and different lettering is indicative of a significant difference between sample means.

	Exothermic Peak		Endothermic Peak			
	Enthalpy (J/g)	**Peak Temperature (°C)**	**Enthalpy of melting (J/g)**	**Peak Temperature (°C)**	**Entropy (J/g·K)**	**ΔG**
Fresh	4.2 ± 2.6 [a]	26.1 ± 1.2 [a]	27.1 ± 8.7 [a]	72.1 ± 2.2 [b]	0.079	4.1
Soaked in DI water	*	*	45.4 ± 0.5 [b]	61.0 ± 4.0 [a]	0.136	5.6
Soaked in 50mM KCl	2.5 ± 1.7 [a]	24.4 ± 1.3 [a]	28.5 ± 6.9 [a]	75.8 ± 1.5 [c]	0.082	4.6

* Indicates peak was not significantly different than baseline

An unusual exothermic peak was observed in the fresh sample but not present in the gel soaked in DI water. A slow-cooled (1 °C/min in the μDSC) HA gellan gel also did not exhibit this exothermic transition. A pre-melting step is common in DSC analysis and may be the reason this peak has not been previously reported. It is proposed the peak represents an ordering or semi-crystallization of the amorphous chains in aggregates. Dissolution of HA gellan chains is not complete after 2 hours of heating and some aggregates of up to 10 chains is expected to be present in the sample (Shinsho et al., 2020). When soaking the gels in water, the aggregates must have dissolved and correspondingly the exothermic peak was not present. A much lower effective concentration and lower ionic solution are reasonable to have caused the breakup.

3.3.2. Temperature dependence of modulus

Rheological tests were used to measure the effect of temperature on the modulus to elucidate the importance of each thermal transition. During heating, the modulus gradually decreased with a steep drop approaching the melting temperatures (Figure 6). Melting temperature by μDSC of 72 and 61 °C for fresh gellan gum and soaked in DI water respectively were in good agreement with the rheologically determined gel melting points. Consistent with theory, the helix-coil transition temperature from DSC aligns with the sol-gel transitions temperature measured with rheology (Flores-Huicochea, Rodríguez-Hernández, Espinosa-Solares, & Tecante, 2013; Yang et al., 2019). Aggregate ordering at 25 °C did not result in a measureable shift during the heating ramp and suggested minimal contribution to the gel modulus (Figure 6).

From these experiments, it was hypothesized the further helix formation was driven by a hydrophobic effect. Orientation of the HA gellan molecule during double helix formation has the glyceryl groups internal to the double helix (Morris, Gothard, Hember, Manning, & Robinson, 1996). Hydrogen bonds are known to occur within the helix (Chandrasekaran, Radha, & Thailambal, 1992) but hydrophobicity of the glyceryl groups may also contribute to the stability of the helix. Increased stability of helices of HA over LA gellan was demonstrated to be from the glyceryl groups internal to the helix (Morris, Gothard, Hember, Manning, & Robinson, 1996). Hydrophobic interactions have been suggested to contribute to chain associations of HA gellan (Tako, Teruya, Tamaki, & Konishi, 2009) but were not examined. The following section will use varying solvents to probe a hypothesized hydrophobic-driven helix-coil transition.

3.3.3. Mixed solution swelling

Mixed solvents of water with glucose and ethanol were used to examine the solvent effects on swelling ratio, Young's Modulus, and strain to fracture (Figure 7). Without added salts, increasing ratios of organic solvents resulted in decreasing swelling ratios following a continuous swelling pattern (Figure 7A). This is explained by the lower dielectric constant of ethanol and glucose than

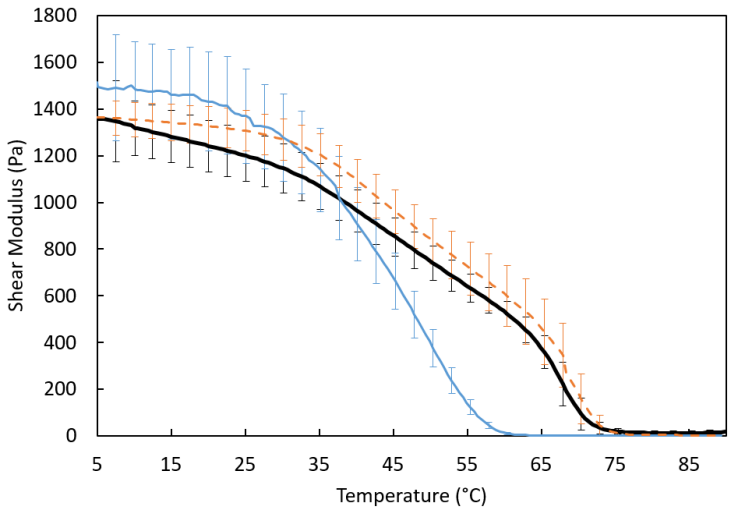

423

424 **Figure 6.** Temperature dependence of storage modulus for 2% high acyl gellan (black) and after
425 soaking in deionized water (blue) and 50mM KCl (dashed orange) utilizing small deformation
426 rheology with controlled heating.

427 water and shown by the high correlation (R^2 = 0.99 for ethanol and R^2 = 0.97 for glucose) between
428 ratio of swelling and dielectric constant of the mixture (Wyman, 1931). For up to 30% of either
429 solvent, there was little effect of the solvent concentration on the modulus, and a slight (20-30%)
430 increase for ethanol compared to pure water. Similar to the effects of salt, the correlation between
431 swelling ratio and modulus was low (R^2 = 0.12 for glucose and R^2 = 0.71 for ethanol) emphasizing a
432 differing underlying mechanisms. Greater ratios of ethanol led to an increasing in modulus but a
433 decrease for glucose. Although not shown on the graph, a 50% ethanol solution resulted in a
434 modulus of 56,000 Pa modulus and was too large to include in Figure 7. Ethanol is thought to
435 decrease swelling and increase the modulus by a de-hydration of the polymer chains (Cassanelli,
436 Norton, & Mills, 2018b). For pectin, the greatest gel strength (rupture force) was also at the point of
437 greatest hydrophobic interactions at 23% ethanol (w/w) (Oakenfull & Scott, 1984). The balance
438 between solubility and molecular interactions are likely both contributing here. At high
439 concentrations of ethanol there was likely a dehydration-based stiffening, while at low
440 concentrations little change was observed.

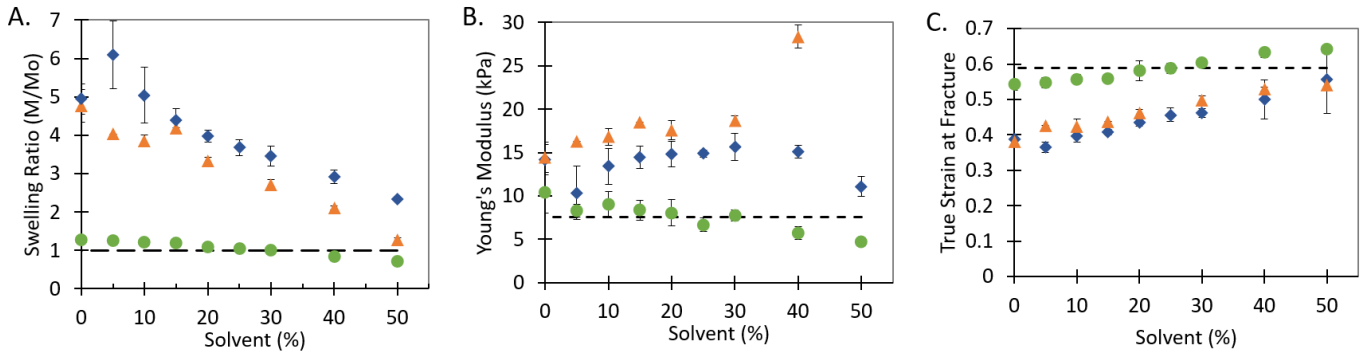

441

442 **Figure 7**. Solvent effects on swelling ratio (A), Young's Modulus (B), and strain at fracture (C) of 2%
443 high acyl gellan gels after soaking in 150mL of water mixed with the indicated percentage of glucose
444 (♦), glucose plus 100mM KCl (●), and ethanol (▲) for 48 hours and compared to a fresh gel (dotted
445 line).

446 To view the effect of glucose without the swelling contribution, a 100 mM KCl concentration was
447 kept constant while changing the ratio of glucose. As intended, the swelling ratio for the glucose
448 mixed solvent with KCl was near to one for every concentration of glucose, although the swelling did
449 decrease with glucose ranging from 1.3 to 0.72 (Figure 7A). When minimizing the swelling, glucose
450 was shown to decrease the modulus and increase the strain to fracture. However there was high
451 correlation between the swelling and modulus (R^2 = 0.88) suggesting swelling was still playing a role
452 in the modulus. For both glucose and ethanol, at low ratios there was little impact of solvent
453 changes on the modulus, but there was a decrease in swelling from the decreasing dielectric
454 constant.

455 Interdependencies between swelling, modulus, and solvent properties are clear from the cumulation
456 of results. The observed swelling of HA gellan gum was consistent with both a swelling process and a
457 de-solvation process. A reduction in salt ions in the surrounding environment appeared to cause
458 both an influx of water by the Donnan effect and a helix-coil transitions. Further testing may allow a
459 better understanding of the properties, but what does seem clear is an importance of both
460 hydrophobic interactions and hydrogen bonds to the gelation of HA gellan gum.

3.4. Importance of swelling in release

If HA gellan is submerged in water prior to use, the texture and water ratios would be vastly different during utilization as shown in section 3.2. Even if the gel was not modified prior to use, during digestion or tissue application the solvent properties of the environment would dictate how the gel responds. It is therefore important to measure the influence of swelling on functionality of the gel. For designing food and drug biomaterials, the effect of the characterized swelling on release of an active molecule is crucial.

A small and uncharged molecule, glucose, was chosen as the drug of interest for these experiments. Release from a similar gelling agent (LA gellan) which displayed a lower ratio of swelling was included as a reference material. Comparison of swelling of the polymers was shown in Figure 1 and the swelling of LA gellan was small (1.1 swelling ratio at 300 minutes). Release profiles of 30% glucose from 2% HA gellan and LA gellan are shown in Figure 8. In DI water, release from HA gellan was considerably slower than LA gellan (at 120 minutes LA gellan was 38% greater) (Figure 8 filled symbols). Under these low ionic conditions, HA gellan swelled considerably during the release experiment (at 120 and 300 minutes a 1.9 and 2.4 swelling ratio respectively). It was hypothesized that swelling decreased release rates of glucose and was tested by conducting the glucose release experiment in ionic conditions that would minimize swelling. Under these ionic conditions (50 mM KCl), the difference between HA and LA gellan was only 17% at 120 minutes (Figure 8 empty symbols). When swelling was inhibited in HA gellan, the release was quicker and more similar to that of the control gel (LA gellan). However, there was still some swelling (1.1 at 120 minutes) which may explain the remaining difference. LA gellan also displayed a small increase in release rate with KCl which corresponded to a decrease in swelling ratio from 1.15 to 1.04 at 120 minutes. Release from HA gellan was quicker when swelling was reduced (in 50 mM KCl) and very similar to LA gellan at comparable swelling ratios. Thus, it was concluded that swelling of HA gellan caused the decreased release rate and the mechanism was subsequently investigated.

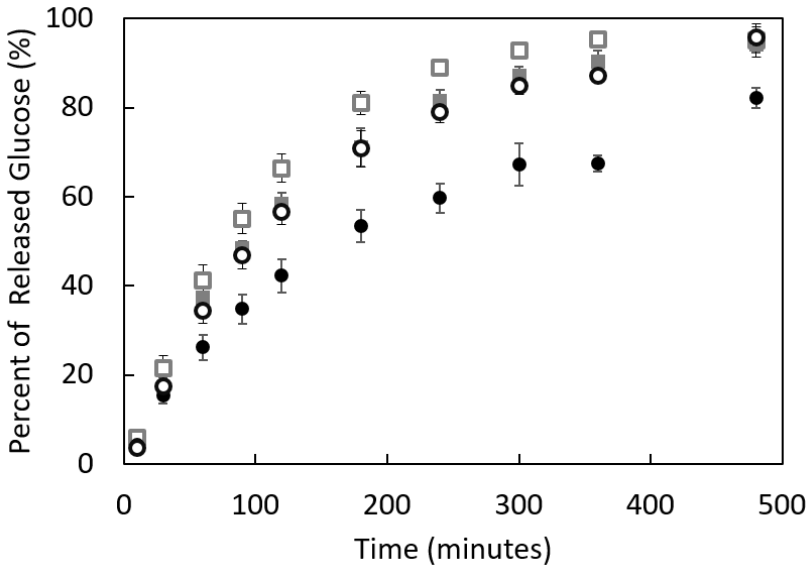

Figure 8. Release of glucose from gels prepared with 30% glucose and 2% high acyl gellan (●) and 2% low acyl gellan (■) into a bulk phase of deionized water (filled symbols) and 50mM KCl (unfilled symbols ○ and □ respectively).

Mesh size of a gel network allows prediction of how compounds of interest would move through the gel. Molecules considerably smaller than the mesh size display little effect to the diffusion through the network, while larger molecules should become trapped in the pores and the release inhibited (Lin & Metters, 2006; Mills, Spyropoulos, Norton, & Bakalis, 2011). Pore size of typical hydrogels in literature range from 100 to 5 nm (Lin & Metters, 2006). Freeze dried HA and LA gellan gum have reported average pore sizes 800-1100 µm and 400-600 µm respectively (Cassanelli, Norton, & Mills, 2018b). Swelling polymers must have structural flexibility and low crosslink density to allow this rearrangement (Moe, Elgsaeter, Skjåk-Bræk, & Smidsrød, 1993). From this understanding, the pore size of both HA and LA gellan is estimated to be much larger than glucose (~1 nm) so trapping in the network pores was unsupported. Additionally, during swelling pores would have increased in size and had the opposite of the observed effect; instead the swelling actually slowed the release.

Network dimensions of these gels suggest glucose was not sterically inhibited during release, so another method was investigated.

In large-pored gels, the effect of a gel network is principally to prevent convection-based mixing so that diffusion is the driving force through the network (Mills, Spyropoulos, Norton, & Bakalis, 2011). Examining the slower release based on the principles of diffusion suggests two possible mechanisms. First, the swelling of the polymer would increase the distance a glucose molecule must travel within the gel to reach the edge. Second, swelling (corresponding to an increase in volume and mass) would lower the effective concentration of glucose inside the gel. Both of these would have caused a lower flux and the slower measured release of glucose from the HA gellan. The decreased flux of glucose due to swelling was confirmed by the release profile quickening when swelling was inhibited. Increasing dimensions of HA gellan during swelling slowed release of the small molecule glucose.

4. Conclusion

In low ionic strength environments, HA gellan gum gels displayed high swelling and an increased modulus caused by an osmotic imbalance and the effect of slowed release of a model drug was demonstrated. Unlike typical polymers for which swelling increases release of a molecule entrapped in the gel network, the swelling of HA gellan caused a slower release. Magnitude of swelling and the speed generated this unique impact. The unusual swelling ability also provided a structural implication consistent with the previously proposed gelation mechanism of a loose and fibrous network without helix aggregation. Additionally, the swell-strengthening behaviour highlighted the contribution of hydrophobic interactions in helix formation for this hydrocolloid. This work begins to suggest that swelling of HA gellan could be harnessed to capture temperature sensitive compounds into a prefabricated gel under suitable conditions. The high degree of swelling and gel hardening, and the tunability of such with ionic environment, provide many opportunities to use HA gellan as a functional ingredient in biopolymer gels.

Acknowledgements. This research was partially funded by the Engineering and Physical Sciences Research Council [grant number EP/K030957/1], the EPSRC Centre for Innovative Manufacturing in Food.

CRediT Author Statement. Kelsey M. Kanyuck: Conceptualization, Methodology, Formal analysis, Investigation, Writing - original draft**. Tom B. Mills:** Supervision, Writing - review & editing**. Ian T. Norton:** Supervision, Funding acquisition, Writing - review & editing. **Abigail B. Norton-Welch:** Supervision, Funding acquisition, Writing - review & editing.

References

Annaka,M., Ogata Y., & Nakahira T. (2000). Swelling behavior of covalently cross-linked gellan gels. *The Journal of Physical Chemistry B 104*, 6755-6760.

Cassanelli,M., Norton I., & Mills T. (2018a). Interaction of mannitol and sucrose with gellan gum in freeze-dried gel systems. *Food Biophysics* , 1-12.

Cassanelli,M., Norton I., & Mills T. (2018b). Role of gellan gum microstructure in freeze drying and rehydration mechanisms. *Food Hydrocolloids 75*, 51-61.

Chandrasekaran,R., Radha A., & Thailambal V. G. (1992). Roles of potassium ions, acetyl and L-glyceryl groups in native gellan double helix: an X-ray study. *Carbohydrate Research 224*, 1-17.

Chen, B., Cai, Y., Liu, T., Huang, L., Zhao, X., Zhao, M., Deng, X., & Zhao, Q. (2020). Formation and performance of high acyl gellan hydrogel affected by the addition of physical-chemical treated insoluble soybean fiber. *Food Hydrocolloids 101*, 105526.

Coutinho, D. F., Sant, S. V., Shin, H., Oliveira, J. T., Gomes, M. E., Neves, N. M., Khademhosseini, A., & Reis, R. L. (2010). Modified Gellan Gum hydrogels with tunable physical and mechanical properties. *Biomaterials 31*, 7494-7502.

De Silva,D. A., Poole-Warren L. A., Martens P. J., & in het Panhuis M. (2013). Mechanical characteristics of swollen gellan gum hydrogels. *Journal of Applied Polymer Science 130*, 3374-3383.

de Souza,F. S., de Mello Ferreira, I. L., da Silva Costa, M. A., da Costa, M. P. M., & da Silva G. M. (2021). Effect of pH variation and crosslinker absence on the gelling mechanism of high acyl gellan: Morphological, thermal and mechanical approaches. *Carbohydrate Polymers 251*, 117002.

Djabourov, M., Nishinari, K., & Ross-Murphy, S. B. (2013). *Physical Gels from Biological and Synthetic Polymers.* Cambridge: Cambridge University Press.

Flores-Huicochea,E., Rodríguez-Hernández A. I., Espinosa-Solares T., & Tecante A. (2013). Sol-gel transition temperatures of high acyl gellan with monovalent and divalent cations from rheological measurements. *Food Hydrocolloids 31*, 299-305.

559 Hossain, K. S. & Nishinari, K. (2009). Chain release behavior of gellan gels. In M. Tokita & K. Nishinari
560 (Eds.). *Gels: Structures, Properties, and Functions* (pp. 177-186). : Springer.

561 Huang,Y., Singh P. P., Tang J., & Swanson B. G. (2004). Gelling temperatures of high acyl gellan as
562 affected by monovalent and divalent cations with dynamic rheological analysis. *Carbohydrate*
563 *Polymers 56*, 27-33.

564 Kasapis,S., Giannouli P., Hember M. W., Evageliou V., Poulard C., Tort-Bourgeois B., & Sworn G.
565 (1999). Structural aspects and phase behaviour in deacylated and high acyl gellan systems.
566 *Carbohydrate Polymers 38*, 145-154.

567 Lin,C. & Metters A. T. (2006). Hydrogels in controlled release formulations: network design and
568 mathematical modeling. *Advanced Drug Delivery Reviews 58*, 1379-1408.

569 Liu,L., Wang B., Gao Y., & Bai T. (2013). Chitosan fibers enhanced gellan gum hydrogels with superior
570 mechanical properties and water-holding capacity. *Carbohydrate Polymers 97*, 152-158.

571 Mazen,F., Milas M., & Rinaudo M. (1999). Conformational transition of native and modified gellan.
572 *International Journal of Biological Macromolecules 26*, 109-118.

573 Mills,T., Spyropoulos F., Norton I. T., & Bakalis S. (2011). Development of an *in-vitro* mouth model to
574 quantify salt release from gels. *Food Hydrocolloids 25*, 107-113.

575 Miyoshi, E. & Nishinari, K. (1999). Rheological and thermal properties near the sol-gel transition of
576 gellan gum aqueous solutions. In Anonymous *Physical Chemistry and Industrial Application of Gellan*
577 *Gum* (pp. 68-82). : Springer.

578 Moe,S. T., Elgsaeter A., Skjåk-Bræk G., & Smidsrød O. (1993). A new approach for estimating the
579 crosslink density of covalently crosslinked ionic polysaccharide gels. *Carbohydrate Polymers 20*, 263-
580 268.

581 Morris,E. R., Gothard M., Hember M., Manning C. E., & Robinson G. (1996). Conformational and
582 rheological transitions of welan, rhamsan and acylated gellan. *Carbohydrate Polymers 30*, 165-175.

583 Morris,E. R., Nishinari K., & Rinaudo M. (2012). Gelation of gellan–a review. *Food Hydrocolloids 28*,
584 373-411.

585 Murillo-Martínez,M.,M. & Tecante A. (2014). Preparation of the sodium salt of high acyl gellan and
586 characterization of its structure, thermal and rheological behaviors. *Carbohydrate Polymers 108*,
587 313-320.

588 Nakamura,K., Shinoda E., & Tokita M. (2001). The influence of compression velocity on strength and
589 structure for gellan gels. *Food Hydrocolloids 15*, 247-252.

590 Nitta,Y., Ikeda S., & Nishinari K. (2006). The reinfocement of gellan gel network by the immersion
591 into salt solution. *International Journal of Biological Macromolecules 38*, 145-147.

592 Norton,A. B., Hancocks R. D., & Grover L. M. (2014). Poly (vinyl alcohol) modification of low acyl
593 gellan hydrogels for applications in tissue regeneration. *Food Hydrocolloids 42*, 373-377.

Oakenfull,D. & Scott A. (1984). Hydrophobic Interaction in the Gelation of High Methoxyl Pectins. *Journal of Food Science 49*, 1093-1098.

Osmałek,T. Z., Froelich A., Jadach B., & Krakowski M. (2018). Rheological investigation of high-acyl gellan gum hydrogel and its mixtures with simulated body fluids. *Journal of Biomaterials Applications 32*, 1435-1449.

Palumbo,F. S., Federico S., Pitarresi G., Fiorica C., & Giammona G. (2020). Gellan gum-based delivery systems of therapeutic agents and cells. *Carbohydrate Polymers 229*, 115430.

Pereira,D. R., Silva-Correia J., Caridade S. G., Oliveira J. T., Sousa R. A., Salgado A. J., Oliveira J. M., Mano J. F., Sousa N., & Reis R. L. (2011). Development of gellan gum-based microparticles/hydrogel matrices for application in the intervertebral disc regeneration. *Tissue Engineering Part C: Methods 17*, 961-972.

Sakai, T. (2020). *Physics of Polymer Gels.* : John Wiley & Sons.

Shinsho,A., Brenner T., Descallar F. B., Tashiro Y., Ando N., Zhou Y., Ogawa H., & Matsukawa S. (2020). The thickening properties of native gellan gum are due to freeze drying–induced aggregation. *Food Hydrocolloids* , 105997.

Skouri,R., Schosseler F., Munch J. P., & Candau S. J. (1995). Swelling and elastic properties of polyelectrolyte gels. *Macromolecules 28*, 197-210.

Stevens,L. R., Gilmore K. J., & Wallace G. G. (2016). Tissue engineering with gellan gum. *Biomaterials Science 4*, 1276-1290.

Sworn, G. (2009). Gellan gum. In G. O. Phillips & P. A. Williams (Eds.). *Handbook of Hydrocolloids* (pp. 204-227). : Woodhead Publishing Limited.

Tako,M., Teruya T., Tamaki Y., & Konishi T. (2009). Molecular origin for rheological characteristics of native gellan gum. *Colloid and Polymer Science 287*, 1445.

Tanaka,S. & Nishinari K. (2007). Unassociated molecular chains in physically crosslinked gellan gels. *Polymer Journal 39*, 397-403.

Wyman, J. (1931). The dielectric constant of mixtures of ethyl alcohol and water from-5 to 40. *Journal of the American Chemical Society 53*, 3292-3301.

Yang,X., Hou Y., Gong T., Sun L., Xue J., & Guo Y. (2019). Concentration-dependent rheological behavior and gelation mechanism of high acyl gellan aqueous solutions. *International Journal of Biological Macromolecules 131*, 959-970.

Yu,I., Kaonis S., & Chen R. (2017). A study on degradation behavior of 3D printed gellan gum scaffolds. *Procedia CIRP 65*, 78-83.